Lack of riluzole efficacy in the progression of the neurodegenerative phenotype in a new conditional mouse model of striatal degeneration

Grzegorz Kreiner Corresp., [1] , **Katarzyna Rafa-Zabłocka** [1] , **Piotr Chmielarz** [1] , **Monika Bagińska** [1] , **Irena Nalepa** [1]

[1] Institute of Pharmacology, Polish Academy of Sciences, Dept. Brain Biochemistry, Kraków, Poland

Corresponding Author: Grzegorz Kreiner
Email address: kreiner@if-pan.krakow.pl

Background. Huntington's disease (HD) is a rare familial autosomal dominant neurodegenerative disorder characterized by progressive degeneration of medium spiny neurons (MSNs) located in the striatum. Currently available treatments of HD are only limited to alleviating symptoms; therefore, high expectations for an effective therapy are associated with potential replacement of lost neurons through stimulation of postnatal neurogenesis. One of the drugs of potential interest for the treatment of HD is riluzole, which may act as a positive modulator of adult neurogenesis, promoting replacement of damaged MSNs. The aim of this study was to evaluate the effects of chronic riluzole treatment on a novel HD-like transgenic mouse model, based on the genetic ablation of the transcription factor TIF-IA. This model is characterized by selective and progressive degeneration of MSNs.

Methods. Selective ablation of TIF-IA in MSNs (TIF-IA^{D1RCre} mice) was achieved by Cre-based recombination driven by the dopamine 1 receptor (D1R) promoter in the C57Bl/6N mouse strain. Riluzole was administered for 14 consecutive days (5 mg/kg, i.p.; 1x daily) starting at 6 weeks of age. Behavioral analysis included a motor coordination test performed on 13-week-old animals on an accelerated rotarod (4 to 40 r.p.m.; 5 min). To visualize the potential effects of riluzole treatment, the striata of the animals were stained by immunohistochemistry (IHC) and/or immunofluorescence (IF) with Ki67 (marker of proliferating cells), neuronal markers (NeuN, MAP2, DCX), and markers associated with neurodegeneration (GFAP, 8OHdG, FluoroJade C). Additionally, the morphology of dendritic spines of neurons was assessed by a commercially available FD Rapid Golgi Stain™ Kit.

Results. A comparative analysis of IHC staining patterns with chosen markers for the neurodegeneration process in MSNs did not show an effect of riluzole on delaying the progression of MSN cell death despite an observed enhancement of cell proliferation as visualized by the Ki67 marker. A lack of a riluzole effect was also reflected by the behavioral phenotype associated with MSN degeneration. Moreover, the analysis of dendritic spine morphology did not show differences between mutant and control animals.

Discussion. Despite the observed increase in newborn cells in the subventricular zone (SVZ) after riluzole administration, our study did not show any differences between riluzole-treated and non-treated mutants, revealing a similar extent of the neurodegenerative phenotype evaluated in 13-week-old TIF-IA^{D1RCre} animals. This could be due to either the treatment paradigm (relatively low dose of riluzole used for this study) or the possibility that the effects were simply too weak to have any functional meaning. Nevertheless, this study is in line with others that question the effectiveness of riluzole in animal models and raise concerns about the utility of this drug due to its rather modest clinical efficacy.

Author Cover Page

Lack of riluzole efficacy in the progression of the neurodegenerative phenotype in a new conditional mouse model of striatal degeneration

Grzegorz Kreiner[1#], Katarzyna Rafa-Zabłocka[1], Piotr Chmielarz[1], Monika Bagińska[1], Irena Nalepa[1]

[1]Institute of Pharmacology, Polish Academy of Sciences, Dept. Brain Biochemistry,

31-343 Kraków, Smętna street 12, Poland

[#]Corresponding Author:

Grzegorz Kreiner

e-mail: kreiner@if-pan.krakow.pl

Abstract

Background. Huntington's disease (HD) is a rare familial autosomal dominant neurodegenerative disorder characterized by progressive degeneration of medium spiny neurons (MSNs) located in the striatum. Currently available treatments of HD are only limited to alleviating symptoms; therefore, high expectations for an effective therapy are associated with potential replacement of lost neurons through stimulation of postnatal neurogenesis. One of the drugs of potential interest for the treatment of HD is riluzole, which may act as a positive modulator of adult neurogenesis, promoting replacement of damaged MSNs. The aim of this study was to evaluate the effects of chronic riluzole treatment on a novel HD-like transgenic mouse model, based on the genetic ablation of the transcription factor TIF-IA. This model is characterized by selective and progressive degeneration of MSNs.

Methods. Selective ablation of TIF-IA in MSNs (TIF-IA^{D1RCre} mice) was achieved by Cre-based recombination driven by the dopamine 1 receptor (D1R) promoter in the C57Bl/6N mouse strain. Riluzole was administered for 14 consecutive days (5 mg/kg, i.p.; 1x daily) starting at 6 weeks of age. Behavioral analysis included a motor coordination test performed on 13-week-old animals on an accelerated rotarod (4 to 40 r.p.m.; 5 min). To visualize the potential effects of riluzole treatment, the striata of the animals were stained by immunohistochemistry (IHC) and/or immunofluorescence (IF) with Ki67 (marker of proliferating cells), neuronal markers (NeuN; microtubule-associated protein-2, MAP2; doublecortin, DCX), and markers associated with neurodegeneration (GFAP, 8OHdG, FluoroJade C). Additionally, the morphology of dendritic spines of neurons was assessed by a commercially available FD Rapid Golgi Stain™ Kit.

Results. A comparative analysis of IHC staining patterns with chosen markers for the neurodegeneration process in MSNs did not show an effect of riluzole on delaying the progression of MSN cell death despite an observed enhancement of cell proliferation as visualized by the Ki67 marker. A lack of a riluzole effect was also reflected by the behavioral phenotype associated with MSN degeneration. Moreover, the analysis of dendritic spine morphology did not show differences between mutant and control animals.

Discussion. Despite the observed increase in newborn cells in the subventricular zone (SVZ) after riluzole administration, our study did not show any differences between riluzole-treated and

non-treated mutants, revealing a similar extent of the neurodegenerative phenotype evaluated in 13-week-old TIF-IA^{D1RCre} animals. This could be due to either the treatment paradigm (relatively low dose of riluzole used for this study) or the possibility that the effects were simply too weak to have any functional meaning. Nevertheless, this study is in line with others that question the effectiveness of riluzole in animal models and raise concerns about the utility of this drug due to its rather modest clinical efficacy.

Introduction

Huntington's disease (HD) is a rare (1:10000) familial autosomal dominant neurodegenerative disorder caused by an expanded stretch of polyglutamine (polyQ) repeats in the protein huntingtin (Hannan 2005) and characterized by progressive degeneration of medium spiny neurons (MSNs) located in the striatum. The disease inevitably culminates with death and cures to at least retard its progression are unavailable so far. Currently available treatments are limited to alleviating some of the symptoms, mainly involuntary movements, associated with the disease. Despite the known origin, there is a lack of understanding of the complex pathogenesis of HD, which affects multiple functions and regulatory pathways, making the development of efficient therapeutics challenging (Kazantsev & Hersch 2007). Classic pharmacological models of HD are based on applying a neurotoxin, 3-nitropropionic acid (3-NP) (Tunez et al. 2010), however this approach leads to immediate neuronal death, which substantially narrows the opportunity to observe the pathological changes associated with the slow neurodegenerative process. On the other hand, many transgenic animal models of HD, even though created by replicating the same genetic malfunction directly responsible for HD in humans, do not fully recapitulate the HD-like phenotype, including profound neuronal loss (or at least not to the expected extent) (Kreiner 2015).

Designed cell therapies for neurodegenerative diseases are mostly based on the replacement of lost neurons through transplantation or activation of neuronal progenitor cells (Emsley et al. 2005). In rodent models of HD, induced neurogenesis in MSNs is thought to be evoked primarily due to neuronal precursors derived from the subventricular zone (SVZ) of the lateral ventricles. The SVZ represents the largest reservoir of adult stem-like progenitors and in normal conditions gives rise to new olfactory bulb interneurons (Bonfanti & Peretto 2007). Stimulation of postnatal neurogenesis is being considered as a potential therapeutic target in several neurodegenerative diseases including HD (Abdipranoto et al. 2008; Lindvall & Kokaia 2010; Ransome et al. 2012). One of the drugs of potential interest for the treatment of HD is riluzole, already approved for the treatment of amyotrophic lateral sclerosis (ALS) (Miller et al. 2012). Riluzole, by interfering with glutamatergic neurotransmission, reduces excitotoxicity and acts as a positive modulator of adult neurogenesis, promoting replacement of damaged MSNs, however, whether it has any clinical meaning remains not clear (Katoh-Semba et al. 2002; Squitieri et al. 2008; Veyrac et al. 2009). It was also shown that riluzole treatment can result in

enhancement of damaged neurite formation potentially leading to functional recovery of motoneurons in rat model of L4-6 root avulsion (Bergerot et al. 2004). Based on experimental data coming from cell and animal research, the classic pharmacological mechanism of its action is related to so-called excitotoxic hypothesis of neurodegeneration. Namely, riluzole can inhibit the release of glutamic acid most likely due to the inactivation of voltage-dependent sodium channels on glutamatergic nerve terminals, as well as activation of a G-protein-dependent signaling pathways (Doble 1996). Another postulated mechanism associated with beneficial role of riluzole application is related to observed increase of serum concentrations of brain-derived neurotrophic factor (BDNF) (Katoh-Semba et al. 2002), which neurotrophic factor is known to be significantly diminished in the brains of HD patients, and its level seems to be correlated with diseases onset progression and severity (Gauthier et al. 2004). Moreover, riluzole was shown to be effective in attenuating several clinically relevant symptoms in a variation of an animal MPTP model representing the early phase of Parkinson's disease (PD) (Verhave et al. 2012). Nevertheless, there are still concerns about its utility due to rather modest clinical efficacy (Miller et al. 2012).

To address this question, we applied a novel approach using a mouse model of HD-like phenotype, based on the activation of an endogenous suicide mechanism achieved by genetic ablation of the transcription factor TIF-IA, an essential regulator of polymerase I activity (Kreiner et al. 2013). Inactivation of TIF-IA blocks the synthesis of ribosomal RNA, leading to nucleolar disruption and p53-mediated apoptosis (Yuan et al. 2005). Loss of TIF-IA in neuronal progenitor cells results in mice born without a brain (Parlato et al. 2008), but when it is lost in mature neurons, the major features of the neurodegenerative process are recapitulated. Namely, inactivation of the TIF-IA gene in striatal MSNs (TIF-IA^{D1RCre} mice) recapitulates the phenotypic alterations associated with selective striatal neurodegeneration (occurring in 13-week-old mice), including increased oxidative damage and inflammatory response, finally leading to MSN cell death and resulting in an HD-like phenotype (Kreiner et al. 2013). In particular we have shown that 13-week-old TIF-IA^{D1RCre} mice were characterized by profoundly enhanced expression of astro- and microglia markers (GFAP, CD11b), several oxidative stress markers (8-hydroxydeoxyguanosine, 8-OHdG; nitrosylated tyrosine, NITT, neuroketals, NK) as well as TUNEL+ cells. The MSNs cells were progressively lost over the time as visualized by NeuN and D1R immunohistochemical stainings. These cellular events were associated with

motor impairment assessed by rotarod and clasping behavior (Kreiner et al. 2013). In contrast to the majority of other models of neurodegeneration, TIF-IA^{D1Cre}-mutant mice are characterized by the progressive degeneration of targeted neurons over a long period of time (several weeks), mimicking the typical hallmark of the disease (Kreiner et al. 2013).

Materials & Methods

The summary of experimental design is illustrated on the chart (**Fig. 1**).

Mice

Selective ablation of TIF-IA in the MSNs (TIF-IA^{D1RCre} mice) was achieved by *Cre/loxP* recombination in the C57Bl/6N mouse strain. Transgenic mice hosting Cre recombinase under the dopamine 1 receptor (D1R) promoter were crossed with animals harboring the floxed TIF-IA gene as described previously (Kreiner et al. 2013). Mutant TIF-IA^{D1RCre} mice were kept together with their control (Cre-negative) littermates in self-ventilated cages (Allentown, USA) under standard laboratory conditions (12 h light/dark cycle, food and water ad libitum). This study was carried out in strict accordance with the recommendations in the Guide for the Care and Use of Laboratory Animals of the National Institutes of Health. The protocol for the behavioral study was approved by the Animal Ethical Committee at the Institute of Pharmacology, Polish Academy of Sciences (Permit Number: 951, issued: June 28, 2012).

Drug treatment

After genotyping, the 6-week-old mice were divided into 4 experimental groups: control+VEH (con/VEH), control+RIL (con/RIL), mutant+VEH (mut/VEH), mutant+RIL (mut/RIL), receiving either riluzole (RIL; 5 mg/kg, i.p.; Sigma-Aldrich Chemical Co., St. Louis, USA) or vehicle (VEH; 10% DMSO) for 14 consecutive days (1x daily). These doses did not influence daily cage normal behavior observed in riluzole and vehicle treated mice.

Behavioral analysis

A coordination test was performed on 13-week-old animals on an accelerated rotarod (Ugo Basile, Italy). The assessment was preceded by training session, 1 day before the experiment (5 minutes on the rotating rod, constant speed). During the experiment the time spent on the accelerating rod (4 to 40 r.p.m. within 5 min) was measured. Additionally, the weight of the animals was consistently monitored during the time of drug application and on the day before the behavioral test.

Immunohistochemistry

To visualize the potential effects of drug treatment, the striata of animals were subject to *post-mortem* staining using immunohistochemistry (IHC) and/or immunofluorescence (IF) with specific markers as described previously (Chmielarz et al. 2013; Kreiner et al. 2013). Briefly, the mice were sacrificed by cervical dislocation, and their brains were excised, fixed overnight in 4% paraformaldehyde (PFA), dehydrated, embedded in paraffin and sectioned on a rotary microtome on 7 μm thick slices. Chosen sections from corresponding regions of the striatum in mutant and control animals were incubated overnight at 4 °C with primary anti-NeuN (1:500, Millipore; cat. no MAB377), anti-MAP2 (1:1000, Abcam; cat. no ab5392), anti-doublecortin (DCX) (1:100, Abcam; cat. no ab135349), anti-GFAP (1:500, Millipore, cat. no AB5541), and anti-8OHdG (1:200, Millipore; cat. no AB5830) antibodies. Visualization of antigen-bound primary antibodies was carried out using a proper biotinylated secondary antibody together with the Avidin–Biotin Complex (ABC; Vector Laboratories, USA) followed by diaminobenzidine treatment (DAB; Sigma-Aldrich, USA) or an anti-rabbit Alexa-488 or Alexa-594-coupled secondary antibody (Invitrogen, USA). FluoroJade C (Millipore, cat. no AG325) staining was performed according to manufacturer's protocol. Briefly, after deparaffinization and initial incubation in 0.06% KMNO4 (10 min.) the slides were rinsed in distilled water and immersed for 10 min. in 0.001% solution of FluoroJade C dissolved in 0.1% acetic acid vehicle.

Quantification of Ki67 expression was done by counting all Ki67-positive cells on adjacent sections from n=4–6 animals of each genotype/treatment in a single-blind experiment (an investigator did not know which samples belong to which genotype/treatment).

Dendritic spine morphology

Morphological analysis of dendritic spines was assessed as described previously (Chmielarz et al. 2015). Briefly, following extraction, the brains were rinsed in distilled water, impregnated with the use of the FD Rapid Golgi Stain™ Kit (FD NeuroTechnologies, USA), and incubated in 30% sucrose for 3-7 days. Vibratome (Leica, Germany) sections were cut to 100 μm thick and mounted on Super Frost Plus slides (Thermo Scientific, USA) and stained using solutions provided in the kit. The dendritic spines were counted on the dorsal striatum between Bregma 1.1 and 0.0. Dendritic spines were counted on at least 10 μM long fragments of 3rd and 4th row dendrites. There were 3 pieces counted from each neuron and 5 neurons counted for each animal. Only completely stained neurons not obscured by neighboring neurons within the striatum were considered. Spine counting and optical imaging were performed by an experimenter blind to the

genotype of the animal on a Nikon Eclipse 50i (Nikon, Japan) equipped with a CCD camera connected to a computer equipped with NIS Elements BR 30 software.

Statistical analysis

Statistical analysis was performed with Graph Pad Prism 5.01. Data were evaluated by 2-way analysis of variance (2-way ANOVA) followed by Bonferroni test for comparison of biologically relevant groups.

Results

Enhancement of cell proliferation observed in TIF-IA^{D1Cre} mutant mice and after riluzole treatment.

The expression of Ki67 showed substantial enhancement in the region of the SVZ in non-treated 9-week-old TIF-IA^{D1Cre} mice and all riluzole-treated animals (**Fig. 2A-B**). Double immunofluorescent staining revealed that the number of cells labelled with Ki67 (marker of cell proliferation) in SVZ co-localize with the MAP2 (microtubule-associated protein-2, neuronal marker) (**Fig. 2C**) or doblecortin (DCX) positive cells (**Fig. 2D**). These cells co-localize with DAPI (marker for nuclear staining) as well.

Lack of riluzole efficacy on progression of MSNs cell death despite enhancement of cell proliferation.

A comparative analysis of immunohistochemical staining patterns with chosen markers characteristic for neurodegenerative process in MSNs (marker for labeling mature neurons, NeuN; an oxidative stress indicator marker, 8-hydroxydeoxyguanosine, 8OHdG; astrocyte marker, GFAP; marker for degenerating neurons, FluoroJade C) did not show any visual differences between 13-week-old mutant TIF-IA^{D1RCre} mice with or without riluzole treatment (**Fig. 3A-D**). The expression of all of the above-mentioned markers seems to be similar in the riluzole treated and non-treated TIF-IA^{D1RCre}-mutant mice, showing comparable enhancement of inflammatory processes, oxidative stress and neuronal loss.

Lack of riluzole efficacy on the behavioral phenotype associated with MSN degeneration.

Chronic riluzole administration did not prevent impaired motor coordination of 13-week-old mutant TIF-IA^{D1RCre} mice as demonstrated by the rotarod test (**Fig. 4**). The riluzole administration had no effect on control animals, while the different effect of the introduced

mutation is reflected in a 2-way ANOVA, which reveals a treatment (riluzole) x genotype interaction for genotype [$F(131.38) = 80.39$ ($p < 0.0001$)] but not for riluzole itself.

Riluzole does not affect dendritic spine morphology in TIF-IA^{D1RCre} mice.

Our previous research done on TIF-IA^{D1RCre} mice clearly showed that although the neurodegeneration (cell loss) is not observed earlier than in 13-week-old animals, some symptoms of cellular impairment can be seen 2-4 weeks in advance (Kreiner et al. 2013). Taking this into account, we checked whether chronic riluzole treatment could have any positive effects on neural cell morphology. Nevertheless, the performed analysis of the morphology of dendritic spines on 9-week-old animals (where no cell loss is observed yet) did not show any differences between mutants and controls (**Fig. 5**). There was also no effect of riluzole application on dendritic spine morphology in control animals.

Discussion

The objective of this research was supported by preliminary studies, in which we observed an increase in cell proliferation within the SVZ in 9-week-old TIF-IA^{D1RCre} mice suggesting the existence of ongoing neurogenesis (**Fig. 2A-B**). This assumption is consistent with other studies reporting increased neurogenesis in other models of progressive neurodegeneration (Luzzati et al. 2011; Nato et al. 2015). This prompted us that the progressive TIF-IA-driven neurodegeneration in these mice offers the unique advantage to study if, in such conditions, the endogenous progenitors potentially involved in putative neuroprotective mechanisms can be modulated by experimental treatments. However, when performed double staining with Ki67 and NeuN within the SVZ in 9-week-old TIF-IA^{D1RCre} mice, we were not able to find any evidence of co-localization. On the other hand, further immunofluorescent analysis revealed that the number of cells labelled with Ki67 co-localize with the MAP2 or DCX neuronal markers (**Fig. 2C-D**). This may be explained by the fact that DCX and MAP2 belong to early markers of neuronal maturation, while NeuN is a marker of mature neurons being expressed later on (Sarnat 2013).

To elucidate whether the putative further enhancement of cell proliferation, potentially responsible for evoking adult neurogenesis, induced by chronic riluzole administration can have any positive influence on the progression of the neurodegenerative phenotype observed in TIF-IA^{D1RCre} mice, we evaluated chosen markers of neurodegeneration known to be differentially

239 expressed in these mice at 13 weeks old, where the cell loss starts to be clearly visible as
240 described previously (Kreiner et al. 2013). Additionally, we also screened their behavioral
241 phenotype by assessing motor coordination. Despite an observed increase in newborn cells in the
242 SVZ after riluzole administration as visualized by Ki-67 staining (an effective marker of
243 proliferating cells (Kee et al. 2002)) (**Fig. 2**), neither experimental approach showed any
244 differences between riluzole-treated and non-treated mutants, revealing a similar extent of the
245 neurodegenerative phenotype evaluated in 13-week-old animals (**Fig. 3-4**). The mice were
246 characterized by the same expression of induced-GFAP and 8OHdG and profoundly reduced
247 staining intensity for NeuN in the striatum (**Fig. 3A-C**). The neurodegenerative phenotype was
248 further confirmed by FluoroJade C staining, an effective marker of degenerating neurons
249 (Schmued et al. 2005) (**Fig. 3D**). This was reflected by the impairment in motor coordination on
250 the rotarod test, and again, no differences were observed between riluzole- and vehicle-treated
251 mutants (**Fig. 4**). Overall, these experiments did not show any beneficial effects of riluzole
252 administration on the progress of the mutation.
253 It seemed that further enhancement of this process by riluzole administration can bring
254 considerable benefits in the form of slowing down the progression of the mutation. Our
255 transgenic models based on the conditional ablation of transcription factor TIF-IA have already
256 been positively verified as a possible tool to study the mechanisms of action of other
257 pharmacotherapies. In particular, we showed that the progression of neurodegenerative
258 phenotype in the TIF-IA^{DATCre} mice (PD model) can be postponed by L-DOPA (Rieker et al.
259 2011) or reboxetine treatment (Rafa-Zabłocka et al. 2014).
260 It can be argued that either the treatment paradigm was not appropriate to achieve the
261 expected drug efficacy or the effects were simply too weak to have any functional meaning.
262 Regarding the first issue, the dose of riluzole in chronic experiments performed on rodents does
263 indeed range from 1 to 40 mg/kg (Besheer et al. 2009; Carbone et al. 2012; Fumagalli et al.
264 2006; Sepulveda et al. 1999), and is predominantly 20 mg/kg when used to evoke a neurogenesis
265 response. Therefore, the dose used in our experiment was in the lower range of the therapeutic
266 window. The reason for choosing this particular dose was determined by the lethargy and spastic
267 gait followed by a high mortality rate of the mice treated with 20 and 10 mg/kg. This problem
268 has also been reported by other researchers when rats were treated with similar doses and
269 exhibited locomotor ataxia and lethargy (Kitzman 2009; Simard et al. 2012). We presume that

this phenomenon is associated with the specific mouse strain (C57Bl/6N) rather than with the introduced mutation since the problem affected both control and TIF-IA^{D1RCre} mice. Nevertheless, it has to be emphasized that even the dose of 5 mg/kg was able to induce cell proliferation within the SVZ region as visualized by Ki67 staining (**Fig. 2A**) and quantified afterwards (**Fig. 2B**). Moreover, there are existing reports that prove a similar dose to be effective (Kitzman 2009).

In addition, in order to evaluate whether riluzole can exert any influence on affected MSNs, we performed a quantitative analysis of dendritic spine morphology at the stage when the neurons were still present in the striata of TIF-IA^{D1RCre} mice. We analyzed 9-week-old mice, as this is the stage where no cell loss has been observed but the cascade of molecular events leading to degeneration has already been prompted (Kreiner et al. 2013). Nevertheless, this analysis did not show any changes in dendritic spine morphology (**Fig. 5**), supporting the observation that riluzole seems to not be effective in the investigated model.

Surprisingly, we were not able to find any abnormalities in the morphology of dendritic spines in the non-treated TIF-IA^{D1RCre}-mutant mice despite the clear neurodegenerative phenotype that has already been documented. This issue has not been addressed in our previous work. However, the occurrence of such changes is not always correlated with neurodegeneration (Dickstein et al. 2010) or may be a subsequent event. On the other hand, lack of spine pathology might also be attributed to the relatively early stage of pathology observed in 9-week-old TIF-IA^{D1RCre} mutants, as other authors have shown that spine pathology was present in late (36-weeks old) (Spires et al. 2004), but not early (20-weeks old) (Nithianantharajah et al. 2009), symptomatic stages of the R6/1 Huntington disease model.

The lack of analysis of other time points (i.e., 16-week-old animals or older) can be regarded as a drawback of the experimental design. This is mainly due to the relatively low number of animals in the cohort, which is restricted by current strict animal welfare regulations. Nevertheless, since the phenotype of riluzole-treated TIF-IA^{D1RCre} mice is non-distinguishable from untreated mutants (regarding both the behavioral and histological levels) at the age of 13 weeks (where the cells are already starting to degenerate), it would be hard to imagine that any differences would be observed at a later period. Lack of differences at this pivotal stage does not provide any strong support for the investigation of earlier time points, which could have been interesting if we had observed findings differentiating the animals at 13 weeks. However

unlikely, it cannot be excluded that analysis of additional time points in-between 9-th and 13-th week would differentiate the riluzole treated and non-treated animals.

In spite of expectations based on previously gathered evidence in preclinical studies and the use of riluzole in clinics for the treatment of ALS, a recent study also yielded disappointing results concerning this drug. Despite being an expensive drug, it does not stop the progression of ALS and is not always well tolerated, making the efficacy of riluzole in the treatment of ALS inconclusive (Ginsberg & Lowe 2002). Moreover, experiments performed on animal models assessing riluzole as a potential treatment for HD and spinocerebellar ataxia (SCA) had no beneficial effects (Hockly et al. 2006; Schmidt et al. 2016). In clinical trials of anti-HD treatment, there was also no clear neuroprotective effect of riluzole administration, and its effects were narrowed only to reduced chorea (Frank 2014). Thus, our study seems to be in line with others that question the effectiveness of riluzole in animal models and raise concerns about the utility of this drug due to its rather modest clinical efficacy (Limpert et al. 2013).

Conclusions

Despite an observed increase in newborn cells in the SVZ after riluzole administration, our study did not show any differences between riluzole-treated and non-treated mutants, revealing a similar extent of the neurodegenerative phenotype evaluated in 13-week-old TIF-IA^{D1RCre} animals, a new transgenic model resembling HD-like neurodegeneration. This lack of an observed effect could be due to either the treatment paradigm or the possibility that the effects were simply too weak to have any functional meaning. Nevertheless, this study is in line with others that question the effectiveness of riluzole in animal models and raise concerns about the utility of this drug due to its rather modest clinical efficacy.

Acknowledgements

We thank Prof. Günther Schütz and Dr. Rosanna Parlato from the German Cancer Research Center (DKFZ, Heidelberg, Germany) for their generous gift of the TIF-IA^{D1RCre} mice.

Fig. 1. The summary of experimental design. The mice were treated with riluzole (5 mg/kg, i.p.) starting 6-th week of age. The phenotype of riluzole treated vs non-treated animals was compared at 13-th week of age on behavioral and immunohistochemical level, when the effects of the mutation are clearly manifested in neuronal cell loss and behavioral impairment. Ki67 expression and dendritic spines morphology were assessed at 9-th week when cell loss in mutant animals have not yet been observed.

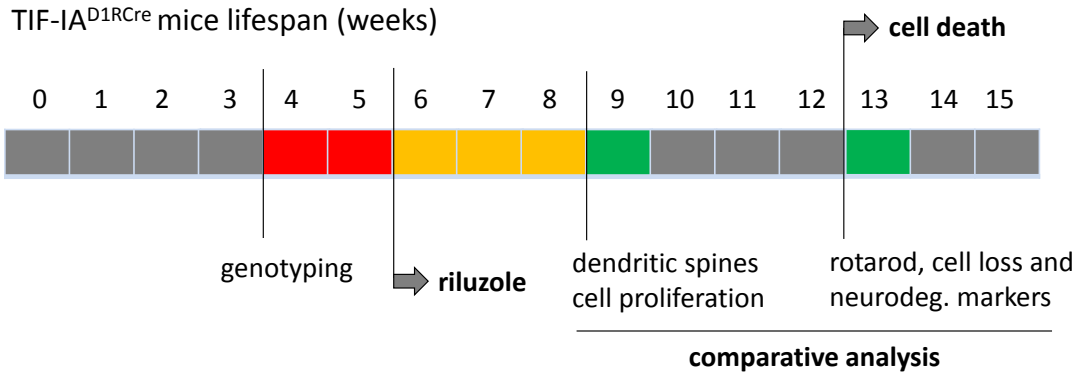

Fig. 2. Representative images of immunofluorescent analysis and quantification of proliferating cells in the region of the SVZ as revealed by the Ki67 marker in control (con) and TIF-IA^{D1RCre}-mutant (mut) riluzole treated and non-treated mice (**A, B**). Example of Ki67/MAP2/DAPI (**C**) or Ki67/DCX/DAPI (**D**) triple-stainings carried out in attempt to confirm nuclear localization and neuronal origin of Ki67 signal (**C**). Numbers of Ki67+ cells are represented by means±S.E.M. (n = 4–6; * $p < 0.05$ vs. con/VEH). RIL – riluzole, VEH – vehicle. Scale bars: 50 µm.

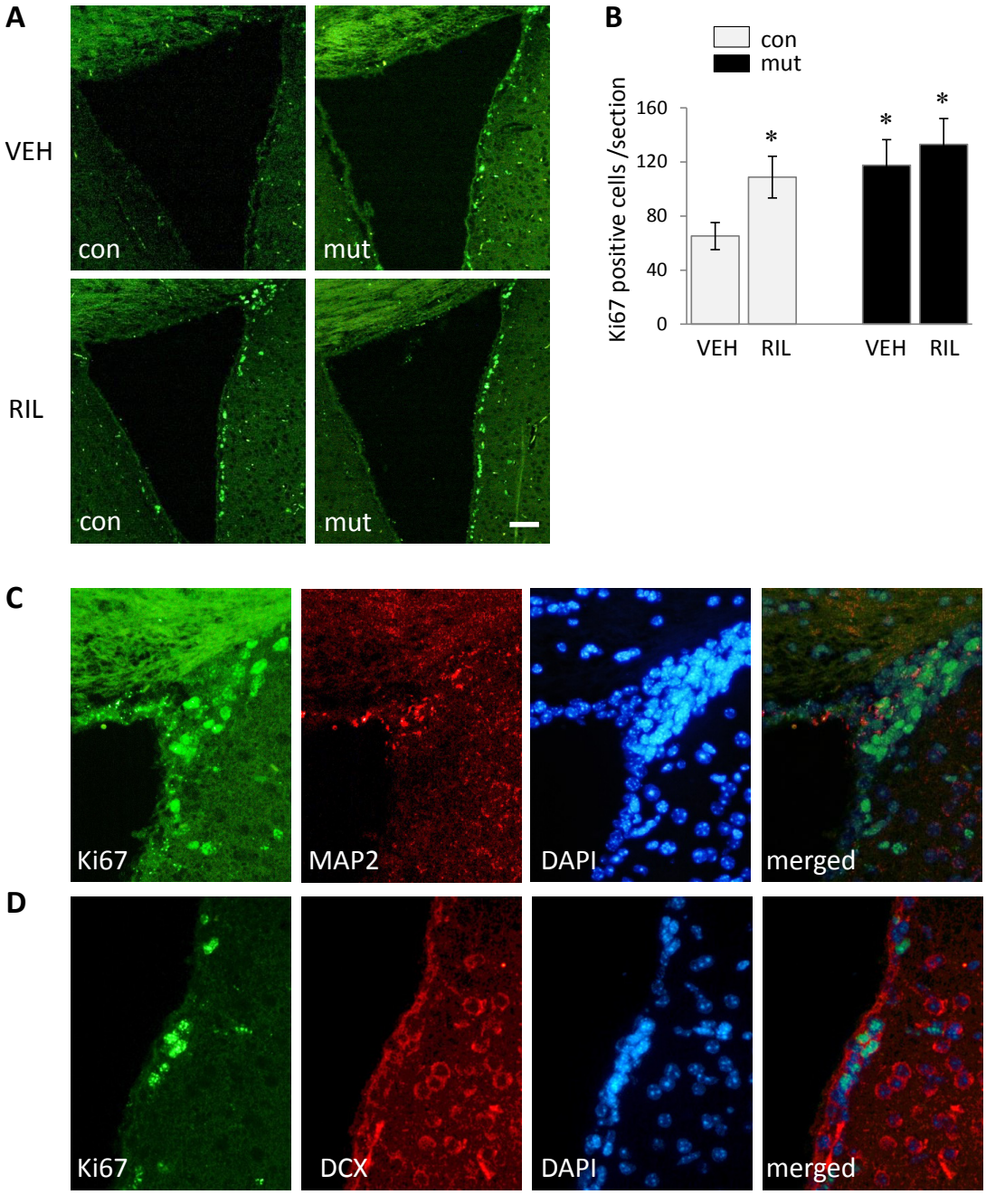

345 **Fig. 3.** Representative images of immunohistochemical analysis showing staining of striata with
346 the NeuN (**A**), induction of oxidative stress detected by the anti-8OHdG antibody **(B)**,
347 astrogliosis visualized by the GFAP-specific antibody **(C)** and degenerating neurons detected by
348 FluoroJade C staining (**D**) in control (con) and TIF-IA^{D1RCre}-mutant (mut) mice. RIL – riluzole,
349 VEH – vehicle. Scale bars: 5 µm (**A, C, D**), 25 µm (**B**).

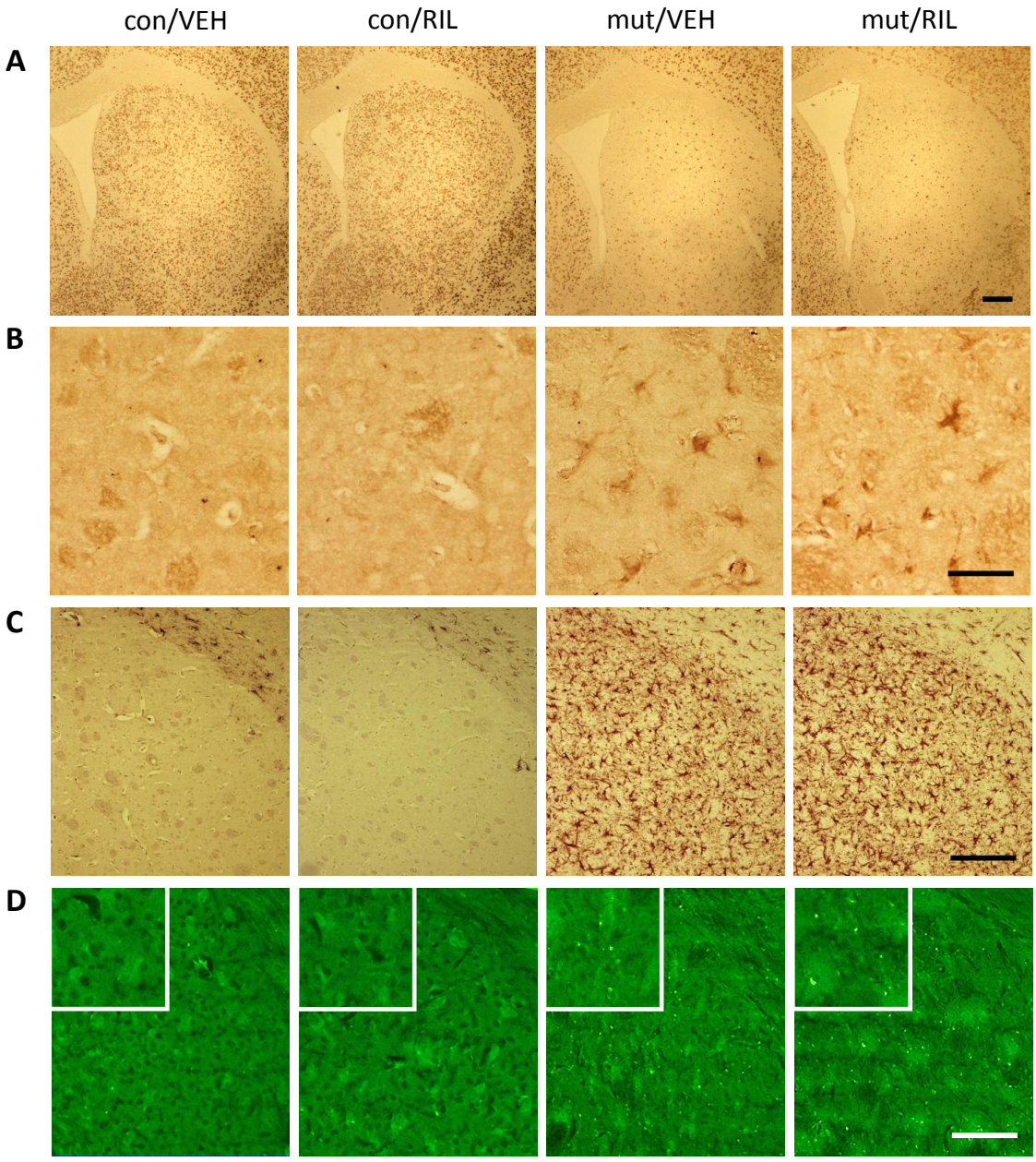

350

351

352 **Fig. 4.** Assessment of motor coordination of control (con) and TIF-IA^{D1RCre}-mutant (mut) mice
353 demonstrated by endurance in the rotarod test. Values for endurance time are represented by
354 means±S.E.M. (n = 7–8; * $p < 0.05$; ** $p < 0.01$ vs. con/VEH). RIL – riluzole, VEH – vehicle.

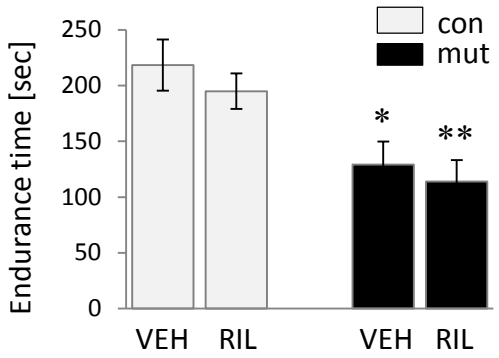

355

356

Fig. 5. Visualization (**A-B**) and quantification (**C**) of dendritic spines in the control (con) and TIF-IA^{D1RCre}-mutant (mut) mice. The spines were counted in the dorsal striatum (Bregma 1.1 – 0.0). Data are represented by the means±SEM (n = 3–4). RIL – riluzole, VEH – vehicle.

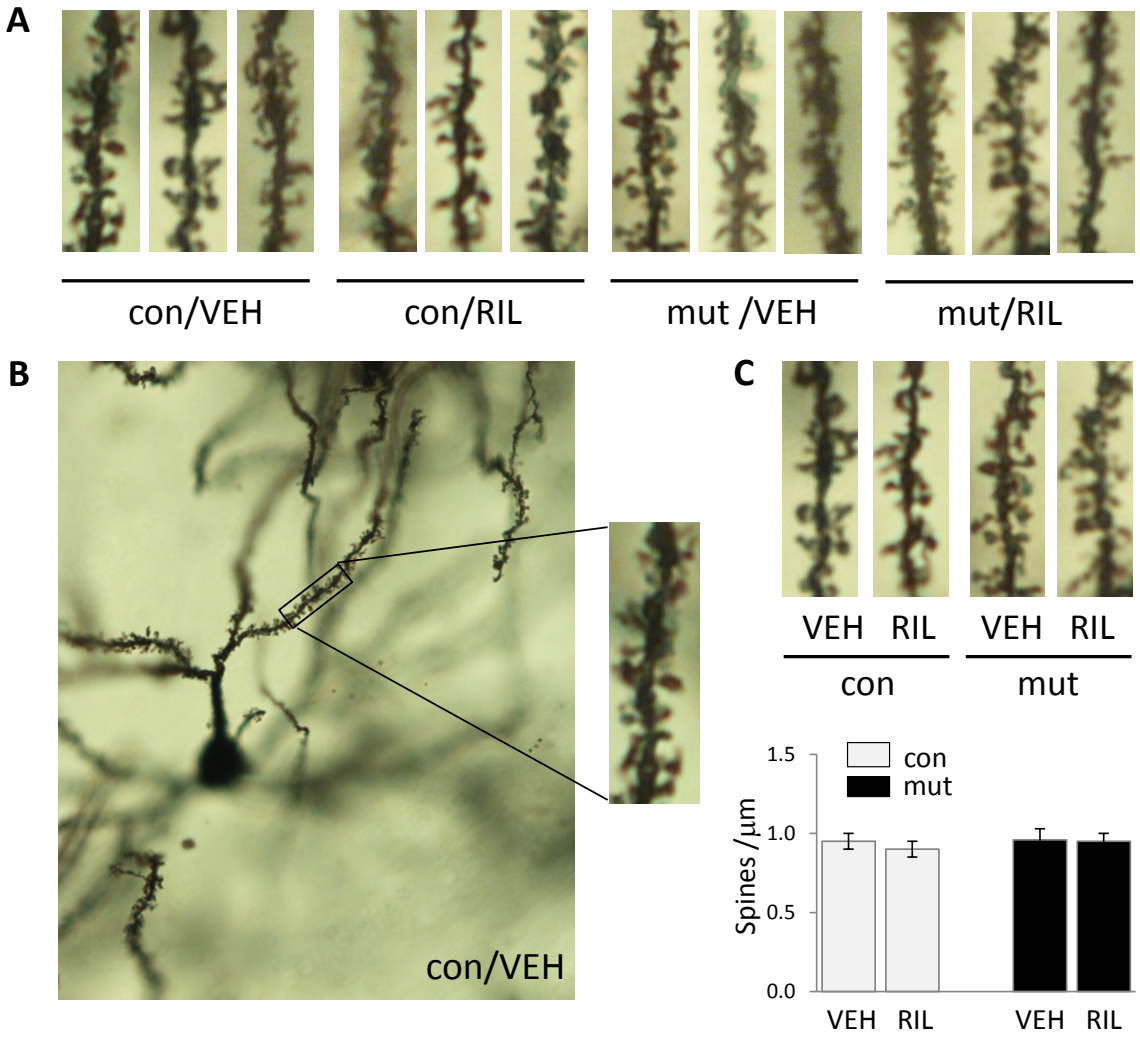

Fig. 5

References

Abdipranoto A, Wu S, Stayte S, and Vissel B. 2008. The role of neurogenesis in neurodegenerative diseases and its implications for therapeutic development. *CNS Neurol Disord Drug Targets* 7:187-210.

Bergerot A, Shortland PJ, Anand P, Hunt SP, and Carlstedt T. 2004. Co-treatment with riluzole and GDNF is necessary for functional recovery after ventral root avulsion injury. *Exp Neurol* 187:359-366.

Besheer J, Lepoutre V, and Hodge CW. 2009. Preclinical evaluation of riluzole: assessments of ethanol self-administration and ethanol withdrawal symptoms. *Alcohol Clin Exp Res* 33:1460-1468.

Bonfanti L, and Peretto P. 2007. Radial glial origin of the adult neural stem cells in the subventricular zone. *Prog Neurobiol* 83:24-36.

Carbone M, Duty S, and Rattray M. 2012. Riluzole neuroprotection in a Parkinson's disease model involves suppression of reactive astrocytosis but not GLT-1 regulation. *BMC Neurosci* 13:38.

Chmielarz P, Kreiner G, Kot M, Zelek-Molik A, Kowalska M, Baginska M, Daniel WA, and Nalepa I. 2015. Disruption of glucocorticoid receptors in the noradrenergic system leads to BDNF up-regulation and altered serotonergic transmission associated with a depressive-like phenotype in female GR(DBHCre) mice. *Pharmacol Biochem Behav* 137:69-77.

Chmielarz P, Kusmierczyk J, Parlato R, Schutz G, Nalepa I, and Kreiner G. 2013. Inactivation of glucocorticoid receptor in noradrenergic system influences anxiety- and depressive-like behavior in mice. *PLoS One* 8:e72632.

Dickstein DL, Brautigam H, Stockton SD, Jr., Schmeidler J, and Hof PR. 2010. Changes in dendritic complexity and spine morphology in transgenic mice expressing human wild-type tau. *Brain Struct Funct* 214:161-179.

Doble A. 1996. The pharmacology and mechanism of action of riluzole. *Neurology* 47:S233-241.

Emsley JG, Mitchell BD, Kempermann G, and Macklis JD. 2005. Adult neurogenesis and repair of the adult CNS with neural progenitors, precursors, and stem cells. *Prog Neurobiol* 75:321-341.

Frank S. 2014. Treatment of Huntington's disease. *Neurotherapeutics* 11:153-160.

Fumagalli E, Bigini P, Barbera S, De Paola M, and Mennini T. 2006. Riluzole, unlike the AMPA antagonist RPR119990, reduces motor impairment and partially prevents motoneuron death in the wobbler mouse, a model of neurodegenerative disease. *Exp Neurol* 198:114-128.

Gauthier LR, Charrin BC, Borrell-Pages M, Dompierre JP, Rangone H, Cordelieres FP, De Mey J, MacDonald ME, Lessmann V, Humbert S, and Saudou F. 2004. Huntingtin controls neurotrophic support and survival of neurons by enhancing BDNF vesicular transport along microtubules. *Cell* 118:127-138.

Ginsberg G, and Lowe S. 2002. Cost effectiveness of treatments for amyotrophic lateral sclerosis: a review of the literature. *Pharmacoeconomics* 20:367-387.

Hannan AJ. 2005. Novel therapeutic targets for Huntington's disease. *Expert Opin Ther Targets* 9:639-650.

Hockly E, Tse J, Barker AL, Moolman DL, Beunard JL, Revington AP, Holt K, Sunshine S, Moffitt H, Sathasivam K, Woodman B, Wanker EE, Lowden PA, and Bates GP. 2006. Evaluation of the benzothiazole aggregation inhibitors riluzole and PGL-135 as therapeutics for Huntington's disease. *Neurobiol Dis* 21:228-236.

404 Katoh-Semba R, Asano T, Ueda H, Morishita R, Takeuchi IK, Inaguma Y, and Kato K. 2002. Riluzole
405 enhances expression of brain-derived neurotrophic factor with consequent proliferation of granule
406 precursor cells in the rat hippocampus. *FASEB J* 16:1328-1330.

407 Kazantsev AG, and Hersch SM. 2007. Drug targeting of dysregulated transcription in Huntington's
408 disease. *Prog Neurobiol* 83:249-259.

409 Kee N, Sivalingam S, Boonstra R, and Wojtowicz JM. 2002. The utility of Ki-67 and BrdU as
410 proliferative markers of adult neurogenesis. *J Neurosci Methods* 115:97-105.

411 Kitzman PH. 2009. Effectiveness of riluzole in suppressing spasticity in the spinal cord injured rat.
412 *Neurosci Lett* 455:150-153.

413 Kreiner G. 2015. Compensatory mechanisms in genetic models of neurodegeneration: are the mice better
414 than humans? *Front Cell Neurosci* 9:56.

415 Kreiner G, Bierhoff H, Armentano M, Rodriguez-Parkitna J, Sowodniok K, Naranjo JR, Bonfanti L, Liss
416 B, Schutz G, Grummt I, and Parlato R. 2013. A neuroprotective phase precedes striatal
417 degeneration upon nucleolar stress. *Cell Death Differ* 20:1455-1464.

418 Limpert AS, Mattmann ME, and Cosford ND. 2013. Recent progress in the discovery of small molecules
419 for the treatment of amyotrophic lateral sclerosis (ALS). *Beilstein J Org Chem* 9:717-732.

420 Lindvall O, and Kokaia Z. 2010. Stem cells in human neurodegenerative disorders--time for clinical
421 translation? *J Clin Invest* 120:29-40.

422 Luzzati F, De Marchis S, Parlato R, Gribaudo S, Schutz G, Fasolo A, and Peretto P. 2011. New striatal
423 neurons in a mouse model of progressive striatal degeneration are generated in both the
424 subventricular zone and the striatal parenchyma. *PLoS One* 6:e25088.

425 Miller RG, Mitchell JD, and Moore DH. 2012. Riluzole for amyotrophic lateral sclerosis (ALS)/motor
426 neuron disease (MND). *Cochrane Database Syst Rev*:CD001447.

427 Nato G, Caramello A, Trova S, Avataneo V, Rolando C, Taylor V, Buffo A, Peretto P, and Luzzati F.
428 2015. Striatal astrocytes produce neuroblasts in an excitotoxic model of Huntington's disease.
429 *Development* 142:840-845.

430 Nithianantharajah J, Barkus C, Vijiaratnam N, Clement O, and Hannan AJ. 2009. Modeling brain reserve:
431 experience-dependent neuronal plasticity in healthy and Huntington's disease transgenic mice. *Am*
432 *J Geriatr Psychiatry* 17:196-209.

433 Parlato R, Kreiner G, Erdmann G, Rieker C, Stotz S, Savenkova E, Berger S, Grummt I, and Schutz G.
434 2008. Activation of an endogenous suicide response after perturbation of rRNA synthesis leads to
435 neurodegeneration in mice. *J Neurosci* 28:12759-12764.

436 Rafa-Zabłocka K, Jurga A, Bagińska M, Parlato R, Schütz G, Nalepa I, and Kreiner G. 2014. Involvement
437 of noradrenergic system in Parkinson's disease – study on novel transgenic mouse models. *Eur*
438 *Neuropsychopharmacol* 24:S642-S643

439 Ransome MI, Renoir T, and Hannan AJ. 2012. Hippocampal neurogenesis, cognitive deficits and
440 affective disorder in Huntington's disease. *Neural Plast* 2012:874387.

441 Rieker C, Engblom D, Kreiner G, Domanskyi A, Schober A, Stotz S, Neumann M, Yuan X, Grummt I,
442 Schutz G, and Parlato R. 2011. Nucleolar disruption in dopaminergic neurons leads to oxidative
443 damage and parkinsonism through repression of mammalian target of rapamycin signaling. *J*
444 *Neurosci* 31:453-460.

445 Sarnat HB. 2013. Clinical neuropathology practice guide 5-2013: markers of neuronal maturation. *Clin*
446 *Neuropathol* 32:340-369.

447 Schmidt J, Schmidt T, Golla M, Lehmann L, Weber JJ, Hubener-Schmid J, and Riess O. 2016. In vivo
448 assessment of riluzole as a potential therapeutic drug for spinocerebellar ataxia type 3. *J*
449 *Neurochem* 138:150-162.

450 Schmued LC, Stowers CC, Scallet AC, and Xu L. 2005. Fluoro-Jade C results in ultra high resolution and
451 contrast labeling of degenerating neurons. *Brain Res* 1035:24-31.

452 Sepulveda J, Astorga JG, and Contreras E. 1999. Riluzole decreases the abstinence syndrome and
453 physical dependence in morphine-dependent mice. *Eur J Pharmacol* 379:59-62.

454 Simard JM, Tsymbalyuk O, Keledjian K, Ivanov A, Ivanova S, and Gerzanich V. 2012. Comparative
455 effects of glibenclamide and riluzole in a rat model of severe cervical spinal cord injury. *Exp*
456 *Neurol* 233:566-574.

457 Spires TL, Grote HE, Garry S, Cordery PM, Van Dellen A, Blakemore C, and Hannan AJ. 2004.
458 Dendritic spine pathology and deficits in experience-dependent dendritic plasticity in R6/1
459 Huntington's disease transgenic mice. *Eur J Neurosci* 19:2799-2807.

460 Squitieri F, Ciammola A, Colonnese C, and Ciarmiello A. 2008. Neuroprotective effects of riluzole in
461 Huntington's disease. *Eur J Nucl Med Mol Imaging* 35:221-222.

462 Tunez I, Tasset I, Perez-De La Cruz V, and Santamaria A. 2010. 3-Nitropropionic acid as a tool to study
463 the mechanisms involved in Huntington's disease: past, present and future. *Molecules* 15:878-
464 916.

465 Verhave PS, Jongsma MJ, Van Den Berg RM, Vanwersch RA, Smit AB, and Philippens IH. 2012.
466 Neuroprotective effects of riluzole in early phase Parkinson's disease on clinically relevant
467 parameters in the marmoset MPTP model. *Neuropharmacology* 62:1700-1707.

468 Veyrac A, Sacquet J, Nguyen V, Marien M, Jourdan F, and Didier A. 2009. Novelty determines the
469 effects of olfactory enrichment on memory and neurogenesis through noradrenergic mechanisms.
470 *Neuropsychopharmacology* 34:786-795.

471 Yuan X, Zhou Y, Casanova E, Chai M, Kiss E, Grone HJ, Schutz G, and Grummt I. 2005. Genetic
472 inactivation of the transcription factor TIF-IA leads to nucleolar disruption, cell cycle arrest, and
473 p53-mediated apoptosis. *Mol Cell* 19:77-87.

474

475